Nonlinear Control of Remote Unstable States in a Liquid Bridge Convection Experiment

Valery Petrov,* Michael F. Schatz,† Kurt A. Muehlner, Stephen J. VanHook, W. D. McCormick, J. B. Swift, and Harry L. Swinney‡

Center for Nonlinear Dynamics and Department of Physics, The University of Texas at Austin, Austin, Texas 78712

(Received 31 July 1996)

We demonstrate the stabilization of unstable periodic orbits whose trajectories in phase space are distant from the unperturbed dynamics in a convective flow experiment. A model independent, nonlinear control algorithm uses temperature measurements near the free surface of a convecting liquid bridge to compute control perturbations which are applied by a thermoelectric element. The algorithm employs a time series reconstruction of a nonlinear control surface to alter the system dynamics. [18S0031-9007(96)01511-6]

PACS numbers: 05.45.+b, 47.20.Dr, 47.20.Ky, 47.54.+r

Understanding of nonlinear dynamical systems has been exploited to control complex behavior in physical, chemical, and biological systems [1–5]; however, the range of control has typically been restricted to targeting unstable states that are near the unperturbed (autonomous) behavior of the system. In all these cases, control of chaotic dynamics has been implemented using OGY (Ott-Grebogi-Yorke) [6] and related low-dimensional linear methods [7–9] which rely on ergodicity to bring the system state near to the desired orbit before control is applied. If the target states are far from the attractor of the unperturbed system, linear methods fail because they do not correctly describe the large feedback perturbations that are necessary for control [10].

In this Letter we report the first example of stabilization of an isolated unstable state in a laboratory experiment. Unstable states distant in phase space from the attractor of a system arise frequently in nonlinear dynamics. For example, trajectories on a toroidal (quasiperiodic) attractor never approach the unstable limit cycle that gave birth to the torus at a secondary Hopf bifurcation [11]. Thus the unstable limit cycle cannot be captured by using small perturbations. We target unstable periodic orbits isolated from dynamics on a torus in a liquid bridge convection experiment using a nonlinear control algorithm that permits perturbations of large amplitude [12]. The algorithm requires no knowledge of the underlying nonlinear equations governing the fluid flow.

A liquid bridge is formed by trapping a liquid between two coaxial cylindrical boundaries [Fig. 1(a)]. Liquid bridge convection models hydrodynamic effects in the float-zone refinement of crystalline materials, where the appearance of time-dependent convective flow induces undesired variation in the chemical composition of processed crystals [13]. Successful application of control methods to suppress time-dependent flow could produce crystalline materials of higher quality.

Our liquid bridge is composed of purified silicone oil [14] with a Prandtl number of approximately 40 and a volume of 0.065 cm^3. A temperature difference ΔT between the boundaries drives a flow in the bridge by inducing a variation of surface tension σ at the gas-liquid interface. Typically we impose $\Delta T \sim 15$ °C with the upper boundary warmer than the lower; the mean temperature of the bottom boundary is 15.0 °C and ΔT is computer-controlled to a precision of ± 0.05 °C.

The dimensionless number that characterizes the surface tension driving is the Marangoni number $M \equiv \sigma_T \Delta T l / \rho \nu \kappa$ with liquid density ρ, kinematic viscosity ν, thermal diffusivity κ, and $\sigma_T \equiv |\frac{d\sigma}{dT}|$. For small M, the convective flow is time independent. For $M \gtrsim 14\,000$ the flow becomes time dependent with a single fundamental frequency [Fig. 1(b)]; at $M \approx 16\,500$, a second frequency appears. We apply our control scheme to this two frequency state at $M = 17\,750$.

The system dynamics is measured by a single sensor and perturbed by a single feedback element [Fig. 1(a)]. The sensor is a 0.03-cm-diameter thermistor that is placed approximately $l/2$ above the lower rod and 0.03 cm from the surface of the liquid. Time series of the sensor resistance are recorded, and the differences x between adjacent local maxima in the series are computed. The feedback element is a 0.1×0.3 cm thermoelectric device that is placed at the same height as the sensor on the opposite side of the liquid bridge [Fig. 1(a)]. Variation of a voltage u changes the feedback element temperature

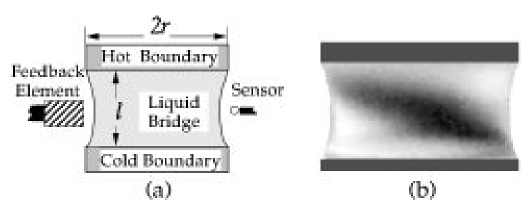

FIG. 1. (a) Sketch of our liquid bridge convection experiment. The boundaries are coaxial stainless steel cylinders with $r = 0.3$ cm and $l = 0.3$ cm. (b) Infrared image of the brightness temperature (darker shading for colder temperatures) for time-periodic liquid bridge convection. The helical structure of the temperature field corresponds to a wave that propagates azimuthally (left to right in the figure).

and imposes a localized perturbation in the surface tension gradients that drive the flow. During the time interval required to determine a given x, the corresponding u is held constant.

Controlling the dynamics requires finding the perturbations that move the system from the present state to the target state. The algorithm proceeds in two stages: *identification* and *control*. During the identification stage uniformly distributed, random perturbations $\overline{u}$ are applied to the liquid bridge, and the corresponding responses $\overline{x}$ are measured to create a reference set. During the control stage, u and x that define the present state are recorded, while u and x for the target state are preset to values determined by the control objective. The reference set is then used to compute the necessary perturbations.

For discrete dynamics at the ith iterate, the next applied perturbation u_{i+1} is given by a control law C

$$u_c(i) \equiv u_{i+1} = C(\mathbf{y}(i)), \qquad (1)$$

where $\mathbf{y}(i)$ is a vector that describes both the present and target states. Figure 2 illustrates schematically how $u_c(i)$ is obtained from $\mathbf{y}(i)$ via the nonlinear mapping C. We will consider the case where $\mathbf{y}(i)$ is constructed from time series x from a single sensor and u from a single perturbing element, although the control law in Eq. (1) can be generalized for the case of multiple sensors and perturbing elements.

For an m-dimensional linear system, the state of a system is sufficiently described in a time-delay space by sequences $\mathbf{u}$ and $\mathbf{x}$, each of length m [12]; we assume that $\mathbf{u}$ and $\mathbf{x}$ of length m are also sufficient to specify m-dimensional dynamics in the weakly nonlinear regime [15]. The present state at the ith iterate is determined by $\mathbf{x}_p(i) \equiv (x_{i-m+1}, \ldots, x_i)$ and $\mathbf{u}_p(i) \equiv (u_{i-m-d+1}, \ldots, u_{i-d})$, where d is a delay which includes the time for an applied perturbation to propagate to the spatially separate sensor. The target state is separated from the present state by $m + d$ iterations and is characterized by time-forwarded sequences $\mathbf{x}_t(i) \equiv (x_{i+m+d+1}, \ldots, x_{i+2m+d})$ and $\mathbf{u}_t(i) \equiv (u_{i+m+1}, \ldots, u_{i+2m})$ after the control sequence is completed. We use these sequences to define $\mathbf{y}(i) \equiv [\mathbf{x}_p(i), \mathbf{u}_p(i), \mathbf{x}_t(i), \mathbf{u}_t(i)]$. The values of x and u between $\mathbf{x}_p$, $\mathbf{u}_p$ and $\mathbf{x}_t$ and $\mathbf{u}_t$, i.e., $(x_{i+1}, \ldots, x_{i+m+d})$ and $(u_{i-d+1}, \ldots, u_{i+m-1})$, describe the trajectory from the present state to the target state; however, only u_{i+1} is computed at the ith iterate; at subsequent iterates, the remaining values of u are determined by updating the control law C.

Figure 2 schematically demonstrates the approximation of C from the reference data accumulated during the identification stage. In the experiment, one thousand perturbations $\overline{u}$ and the corresponding temperature responses $\overline{x}$ are used to form a set of reference sequences $\overline{\mathbf{y}}$ and corresponding $\overline{u}_c$. The points $(\overline{\mathbf{y}}, \overline{u}_c)$ are scattered about the control surface C due to errors in measurement (Fig. 2). During control at time step i, the N nearest neighbors $\overline{\mathbf{y}}(i_k)$, $k = 1, \ldots, N$ to the vector $\mathbf{y}(i)$ are used to compute a linear approximation of C. For an m-dimensional system, a minimum of $N = 4m$ data points is required for a linear approximation; to improve the robustness of the method we set $N = 8m$ and use singular value decomposition to find the $4m$ coefficients of the approximating hypersurface in this over-determined system. The perturbation $u_c(i)$ is then computed and applied. The entire computation procedure takes only 0.2 sec on a 120 MHz Pentium PC; however, the discrete time description of the dynamics forces a one iteration delay (2.3 sec) before the perturbation is applied.

For stabilization of an unstable periodic orbit in the liquid bridge, the target dynamics are given by $\mathbf{x}_t = 0$ and $\mathbf{u}_t = 0$. When the control algorithm is applied to the two-frequency convective flow, the second oscillation is rapidly

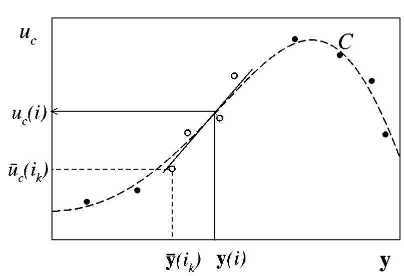

FIG. 2. Schematic representation of the multidimensional control surface C used to determine the next applied feedback perturbation u_c from the present and target states $\mathbf{y}$. In the experiment C is reconstructed from reference points $(\overline{\mathbf{y}}, \overline{u}_c)$ [∘ •] gathered during the identification stage. During control at the ith iterate, nearby points $[\overline{\mathbf{y}}(i_k), \overline{u}_c(i_k)]$ [∘] are used to approximate C for determining $u_c(i)$ from $\mathbf{y}(i)$.

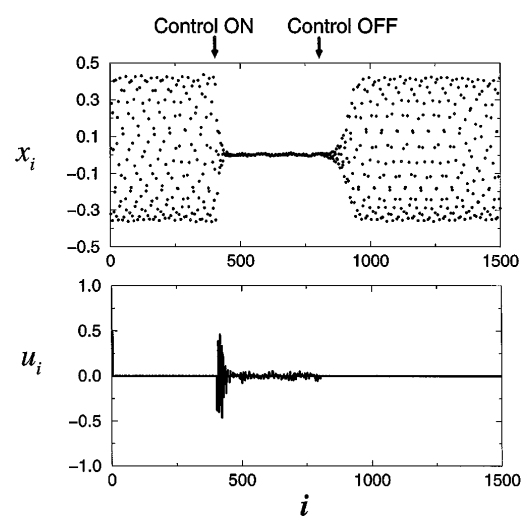

FIG. 3. The application of control is illustrated for discretized dynamics by time series of temperature differences x_i (top) and applied perturbations u_i (bottom). The control is applied at time step $i = 400$ and the second oscillation in the two-frequency state is rapidly suppressed. Removing the control at time step $i = 800$ allows the system to rapidly return to the unperturbed dynamics.

suppressed (Fig. 3). Initially, the applied perturbations are large; at $i = 400$ the root-mean-squared power applied to the thermoelectric element is approximately 10 mW, which is comparable to the heat flow through the liquid bridge due to the temperature difference applied to the boundaries. However, once the periodic orbit is stabilized ($\sim 500 < i < 800$), the thermoelectric power drops to about 100 μW, less than 1% of the heat flow through the bridge (Fig. 3). After the control is turned off, the system rapidly returns to the two-frequency dynamics of the unperturbed state.

We attempt control for several different values of m and d, which are free parameters in our algorithm. The fastest convergence is achieved for $m = 4$ and $d = 2$, which suggests two independent frequencies in the unperturbed dynamics. Two dimensions are required to describe the second frequency present in the unperturbed system; the other two dimensions effectively describe the decay of stable modes in the liquid bridge and the thermal relaxation of the feedback element. The delay $d = 2$ is approximately equal to the sum of the calculation delay and the time for waves with azimuthal wave number 1 and period of 2.3 s to propagate from the feedback element location to the sensor location.

Figure 4 demonstrates that our control method is effective for stabilizing states that lie far from the unperturbed dynamics in the phase space. The target dynamics can lie in any region of phase space that can be accessed during the identification stage; $\bar{u}$ must be chosen sufficiently large to move states in phase space over distances comparable to the separation between the isolated unstable orbit and the attractor of the unperturbed system. The control scheme fails for $M \gtrsim 19\,000$ because the dynamics becomes highly nonlinear, and the one thousand points in our reference set become insufficient for good interpolation. More sophisticated methods developed for nonlinear time series prediction [16] may help extend the parameter range for control by improving the approximation of the control surface C.

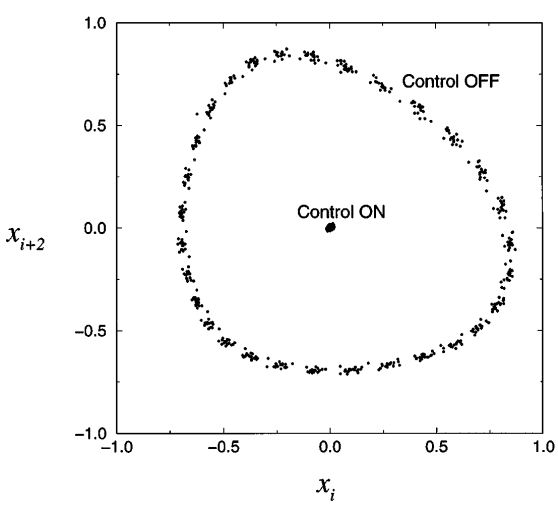

FIG. 4. Second return map constructed from experimental time series illustrating both the toroidal dynamics (control "off") and the stabilized periodic orbit (control "on").

Feedback linearization [17], an alternative approach to nonlinear control, has been demonstrated in low-dimensional nonlinear systems [18]. In this method a feedback loop is constructed specifically to linearize the system dynamics; control is then implemented using standard techniques from linear control theory that adjust the eigenvalues of the closed-loop system. This procedure is sensitive to the errors in parameter estimation from time series and fails as the dimensionality is increased. Our nonlinear control method constructs a control law based on the desired target state rather than on the adjustment of eigenvalues. Comparison of the two methods indicates an order of magnitude higher tolerance to noise for our method as compared to feedback linearization.

Our experiments demonstrate that a single local measurement and feedback perturbation are sufficient to control low-dimensional spatiotemporal dynamics. However, the spatial structure for some states cannot be ignored. In particular, we have attempted to stabilize unstable time-independent states using the present experiment. Oscillations can be suppressed at the sensor location, but infrared imaging reveals the presence of standing waves with antinodes between the feedback element and the sensor. In this case, multiple spatially distributed measurements and perturbations will be required for control; we are presently modifying our control algorithm and experiment to include two sensors and two feedback elements. In this way liquid bridge convection serves as an ideal testbed for methods of controlling spatially extended nonlinear systems.

This research is supported by the NASA Microgravity Science and Applications Division (Grant No. NAG3-1839) and the Office of Naval Research (Grant No. N00014-89-J-1495). S. J. V. H. is supported by the NASA Graduate Student Researchers Program.

*Electronic address: lera@chaos.ph.utexas.edu
†Present address: School of Physics, Georgia Institute of Technology, Atlanta, GA 30332.
Electronic address: schatz@chaos.ph.utexas.edu
‡Electronic address: swinney@chaos.ph.utexas.edu

[1] W. L. Ditto, S. N. Rauseo, and M. L. Spano, Phys. Rev. Lett. **65**, 3211 (1990).
[2] R. Roy, T. W. Murphy, T. D. Maier, Z. Gills, and E. R. Hunt, Phys. Rev. Lett. **68**, 1259 (1992).
[3] V. Petrov, V. Gáspár, J. Masere, and K. Showalter, Nature (London) **361**, 240 (1993).
[4] A. Garfinkel, M. L. Spano, W. L. Ditto, and J. N. Weiss, Science **257**, 1230 (1992).
[5] S. J. Schiff, K. Jerger, D. H. Duong, T. Chang, M. L. Spano, and W. L. Ditto, Nature (London) **370**, 615 (1994).

[6] E. Ott, C. Grebogi, and J. A. Yorke, Phys. Rev. Lett. **64**, 1196 (1990).

[7] K. Pyragas, Phys. Lett. A **170**, 421 (1992).

[8] R. W. Rollins, P. Parmananda, and P. Sherard, Phys. Rev. E **47**, R780 (1993).

[9] B. Peng, V. Petrov, and K. Showalter, J. Phys. Chem. **95**, 4957 (1991).

[10] In some instances unstable states that are originally near a chaotic attractor can be tracked to remote locations using small perturbations. However, this requires a slow variation of the system control parameter(s); if control is lost, the target state can be reacquired only by changing the control parameters to return the system to the original chaotic regime. See, for example, I. Schwartz and I. Triandaf, Phys. Rev. A **46**, 7439 (1992).

[11] P. Berge, Y. Pomeau, and C. Vidal, *Order Within Chaos* (John Wiley, New York, 1986).

[12] V. Petrov and K. Showalter, Phys. Rev. Lett. **76**, 3312 (1996).

[13] A. Croll, W. Muller, and R. Nitsche, Microgravity Sci. Technol. **3**, 204 (1991).

[14] M. F. Schatz and K. Howden, Exp. Fluids **19**, 359 (1995).

[15] For m-dimensional nonlinear systems, sequences $\mathbf{x}$ and $\mathbf{u}$ of length $2m + 1$ may be necessary; see, for example, T. Sauer, J. A. Yorke, and M. Casdagli, J. Stat. Phys. **65**, 579 (1991).

[16] H. D. I. Abarbanel, R. Brown, J. J. Sidorowich, and L. S. Tsimring, Rev. Mod. Phys. **65**, 1331 (1993).

[17] J. Slotine and W. Li, *Applied Nonlinear Control* (Prentice-Hall, Englewood Cliffs, New Jersey, 1991).

[18] C.-C. Fuh and P.-C. Tung, Phys. Rev. Lett. **75**, 2952 (1995).